

# Enrichment of perforate septal pore caps from the basidiomycetous fungus *Rhizoctonia solani* by combined use of French press, isopycnic centrifugation, and Triton X-100

Kenneth G.A. van Driel<sup>a</sup>, Arend F. van Peer<sup>b</sup>, Han A.B. Wösten<sup>b</sup>,  
Arie J. Verkleij<sup>c</sup>, Teun Boekhout<sup>a</sup>, Wally H. Müller<sup>c,\*</sup>

<sup>a</sup> Centraalbureau voor Schimmelcultures (CBS), Royal Netherlands Academy of Arts and Sciences (KNAW), Utrecht, The Netherlands

<sup>b</sup> Molecular Microbiology, Institute of Biomembranes, Utrecht University, Utrecht, The Netherlands

<sup>c</sup> Cellular Architecture and Dynamics, Institute of Biomembranes, Utrecht University, Utrecht, The Netherlands

Received 19 April 2007; received in revised form 11 September 2007; accepted 20 September 2007

Available online 18 October 2007

## Abstract

Septal pore caps occur in many filamentous basidiomycetes located at both sides of the dolipore septum and are at their base connected to the endoplasmic reticulum. The septal pore cap ultrastructure has been described extensively by the use of electron microscopy, but its composition and function are not yet known. To enable biochemical and functional analyses in the future, we here describe an enrichment method for perforate septal pore caps from *Rhizoctonia solani*. Our method is based on the combined use of French press and isopycnic centrifugation, using a discontinuous sucrose gradient followed by a treatment with Triton X-100. Enrichment was monitored by the use of scanning electron microscopy and transmission electron microscopy. Using the same isolation method, smaller septal pore caps were isolated from two other basidiomycetes as well. Furthermore, we showed pore-occluding material co-purified with the septal pore caps. This observation supports the hypothesis that septal pore caps play a key role in the plugging process of the septal pores in filamentous basidiomycetes.

© 2007 Elsevier B.V. All rights reserved.

**Keywords:** Septal pore cap; Basidiomycete; Fungi; *Rhizoctonia solani*; Organelle; Isolation; Isopycnic centrifugation; Electron microscopy; Triton X-100

## 1. Introduction

Filamentous fungi grow by means of hyphae, forming an interconnected network. The hyphae of the higher fungi, i.e. ascomycetes and basidiomycetes (including mushroom-forming fungi and jelly fungi), are regularly septated. The septa have a central pore (Gull, 1978). The ascomycetous septum is tapered towards the pore, whereas the basidiomycetous septum is flared towards the pore, forming the dolipore (Gull, 1978). The septal pore cap (SPC) is a membranous structure located at both sides of the dolipore septum in many basidiomycetes (Girbardt, 1958;

Moore and McAlear, 1962; Bracker and Butler, 1963). In 1958, Girbardt described for the first time the SPC ultrastructure at the septum of *Polystictus versicolor* by the use of transmission electron microscopy (Girbardt, 1958). Since then, many studies on the SPC ultrastructure have followed (e.g. Bracker and Butler, 1963; Patrignani and Pellegrini, 1986; Müller et al., 1998a, 2000b). These studies have shown that the ultrastructure of SPCs is diverse and can be divided into the following main types: the vesicular-tubular type, the imperforate type, and the perforate type (Fig. 1). The absence or presence of a SPC, the SPC-type, and septal morphology are important markers that reflect the main phylogenetic groups of the basidiomycetes (McLaughlin et al., 1995).

Although the ultrastructure of SPCs has been studied extensively, its precise function is still a matter of speculation. As the base of SPCs is continuous with the endoplasmic reticulum (ER), the SPC has been proposed to be a specialized subcompartment of the ER (Girbardt, 1961; Bracker and Butler,

\* Corresponding author. Cellular Architecture and Dynamics, Utrecht University, Padualaan 8, 3584 CH Utrecht, The Netherlands. Tel.: +31 30 2533588; fax: +31 30 2513655.

E-mail address: [w.h.muller@uu.nl](mailto:w.h.muller@uu.nl) (W.H. Müller).

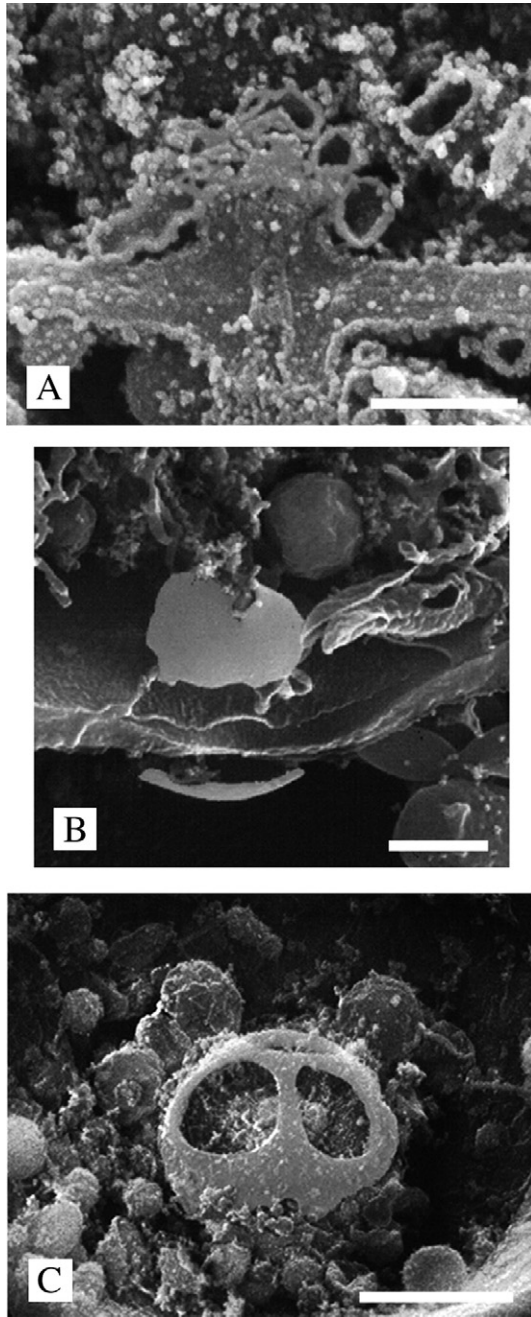


Fig. 1. Scanning electron micrographs of the three main septal pore cap-types that can be associated with the dolipore septum in basidiomycetes. A) A group of vesicular-tubular structures arranged in a hemisphere surrounding the dolipore forms the vesicular-tubular SPC-type (*Trichosporon sporotrichoides*). B) A slightly flattened closed membranous structure forms the imperforate SPC-type (*Epulorhiza anaticula*). C) A dome-shaped structure with perforations forms the perforate SPC-type (*Rhizoctonia solani*). Bars represent 250 nm in A, 500 nm in B, and 1000 nm in C.

1963; Müller et al., 1995a). However, differences in calcium-affinity sites between the ER and SPCs have been observed by the use of zinc–iodine–osmium tetroxide staining (Müller et al., 1995a, 1998a). Possibly, SPCs act as a repository for certain proteins that are produced and processed in the ER, and that are translocated from the SPC to the septal pore when pore sealing is needed in cases of stress or hyphal damage (Müller et al., 1998a).

Several other functions of SPCs have been suggested: they may act as a sieve to discriminate between organelles that pass the pore (Wilsenach and Kessel, 1965), they may guide cytoplasmic streams to the pore (Orlovich and Ashford, 1994), or they may function in protoplasmic streaming, by which SPCs protect the dolipore for accidental closing or diminishing the pore by organelles that could hit the sides of the swelling in case SPCs are absent (Bracker and Butler, 1964). Furthermore, in *Schizophyllum commune*, *Rhizoctonia solani*, and *Pisolithus tinctorius* filamentous structures were observed that connect the inside of the SPC with the pore-occluding material (Orlovich and Ashford, 1994; Müller et al., 2000a). These observations suggest that SPCs play a key role in plug formation after hyphal damage or stress and consequently, are of importance in intercellular communication within the hyphae (Aylmore et al., 1984; Markham, 1994; Müller et al., 2000a).

The many ultrastructural studies of SPCs have led to a number of hypotheses on SPC functioning. Biochemical analysis of SPCs may help further to understand its function in the hyphal cells of basidiomycetes. However, an isolation procedure of SPCs necessary to biochemically study these organelles has never

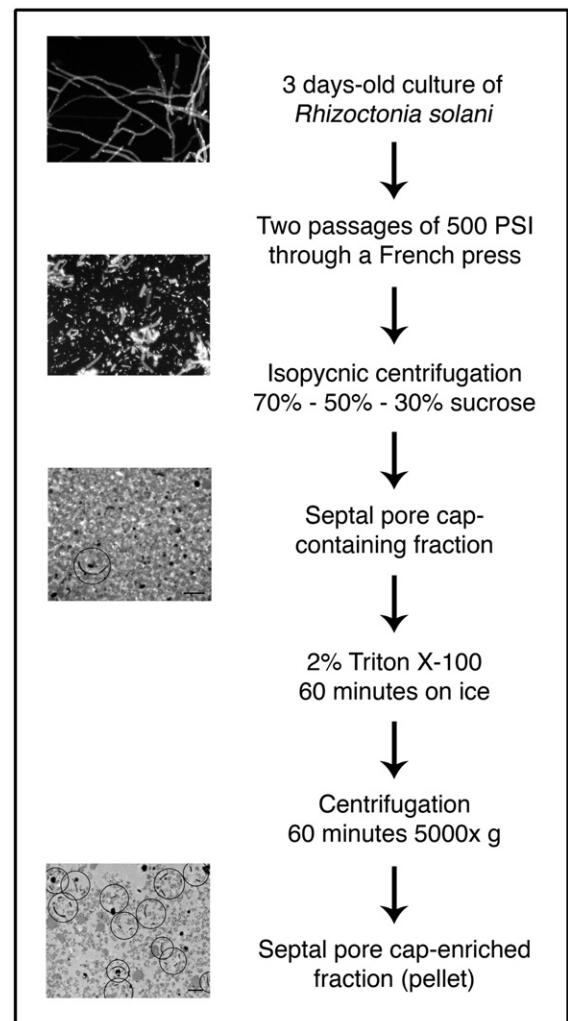


Fig. 2. Flow diagram of the septal pore cap-enrichment procedure.

been published. Therefore, we here describe for the first time a method to enrich SPCs from the basidiomycetous fungus *R. solani*. Using the same procedure, we could also isolate SPCs from two other species belonging to the *Rhizoctonia* sensu lato (s.l.) complex, namely *Thanatephorus cucumeris* and *Ceratobasidium cornigerum*. Furthermore, we showed that a structural complex consisting of SPCs attached by filaments to pore-occluding material could be isolated. The presented method will also allow the future isolation and biochemical analysis of proteins of perforate SPCs from different species of basidiomycetes.

## 2. Materials and methods

### 2.1. Organisms, media and culture conditions

*R. solani* (CBS 346.84), *T. cucumeris* (CBS 700.82), and *C. cornigerum* (CBS 132.82) were grown on malt extract agar (Oxoid) at 25 °C for 4 days. A Sorvall omni-mixer (Kendro Laboratory Products) was used for 1 s at speed 4 to homogenize the culture in 100 ml complete medium (CM) (20.0 g glucose, 2.0 g peptone L37 (Oxoid), 2.0 g yeast extract (Difco), 0.5 g MgSO<sub>4</sub>·7H<sub>2</sub>O, 0.46 g KH<sub>2</sub>PO<sub>4</sub>, 1.0 g K<sub>2</sub>HPO<sub>4</sub>/l) containing 100 mg/l Penicillin-G (Yamanouchi Pharma) and 100,000 units/l Streptomycin (Radiumfarma-Fissiopharma). After growing for 48 h at 175 rpm and 25 °C, the culture was again homogenized. Thereafter, 10 ml of this homogenate was used to inoculate 100 ml CM and growth was allowed for 3 days at 175 rpm and 25 °C.

### 2.2. Subcellular fractionation by isopycnic centrifugation

The mycelium from three-days old submerged cultures was harvested by centrifugation at 2000 rpm and 4 °C for 3 min in a Mistral 400 centrifuge (MSE Scientific Instruments). Subsequently, the mycelium was washed twice in HEPES/KAc (HK) buffer (20 mM HEPES, pH 6.8, 50 mM potassium acetate (KAc),

200 mM D-sorbitol, 1 mM EDTA) (Rieder and Emr, 2000) and resuspended in half a volume of HK buffer supplemented with 1/200 volume of protease inhibitor cocktail (Sigma-Aldrich). The mycelium was disrupted by two passages of 500 psi (equivalent to 3447 kPa) through a French press (American Instrument Company). Twelve ml of fungal cell extract was layered on top of a discontinuous gradient consisting of 8 ml 70% (w/v), 8 ml 50% (w/v), and 8 ml 30% (w/v) sucrose in HK buffer. After centrifugation at 85,000 ×g and 4 °C for 90 min in a Centrikon T-2180 ultracentrifuge (Kontron Instruments), fractions were collected from underneath using a Pasteur pipette with a 180° bent tip. The fractions were diluted with HK buffer containing 2% (w/v) Triton X-100 (GE Healthcare) to a final sucrose concentration of 10% (w/v). After 1 h on ice, fractions were centrifuged at 5000 ×g and 4 °C for 60 min. The resulting pellet was resuspended in 1.0 ml HK buffer and further processed for electron microscopy as described below. To analyze the supernatant (after 5000 ×g centrifugation) for the presence of SPCs, the supernatant was centrifuged at 100,000 ×g and 4 °C for another 45 min. The resulting pellet was resuspended in 1.0 ml HK buffer and processed for electron microscopy. A flow chart of the SPC-enrichment procedure is presented in Fig. 2.

### 2.3. Transmission electron microscopy

For chemical fixation, samples were fixed in 1.5% glutaraldehyde (Agar Scientific Ltd.) buffered with 20 mM HEPES, pH 6.8, overnight at 4 °C. Samples were post-fixed in 1% (w/v) aqueous osmium tetroxide (EMS) for 1 h at room temperature. Subsequently, the samples were gradual dehydrated in a series of ascending concentrations of acetone, and 3 times of 100% acetone containing 1% (v/v) acidified 2,2-dimethoxypropane (DMP) for 30 min each. The samples were gradually infiltrated in Spurr's resin (Spurr, 1969). Finally, the samples were embedded in freshly prepared 100% Spurr's resin and polymerized at 65 °C for 48 h in BEEM capsules (EMS).

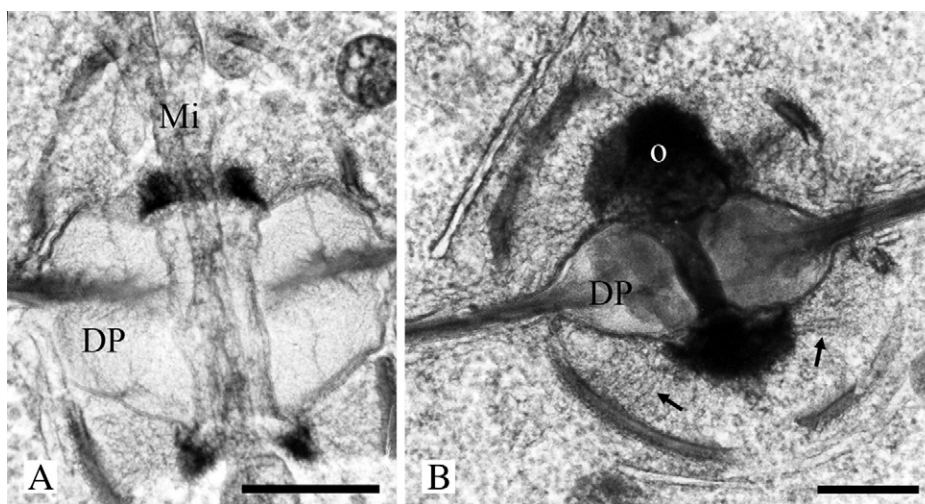


Fig. 3. Transmission electron micrograph of thick 350 nm sections of the dolipore septum in a high-pressure frozen, freeze-substituted and lowicryl HM20 embedded hypha of *Rhizoctonia solani* showing septal pore caps (SPCs) at both sides of the dolipore (DP). The dolipore channel may be open, allowing passage of mitochondria (A) or the dolipore channel can be plugged with electron-dense occluding material (B). Filaments (arrows) are present between SPCs and the plugging material. O = occluding material. Bar represents 500 nm.

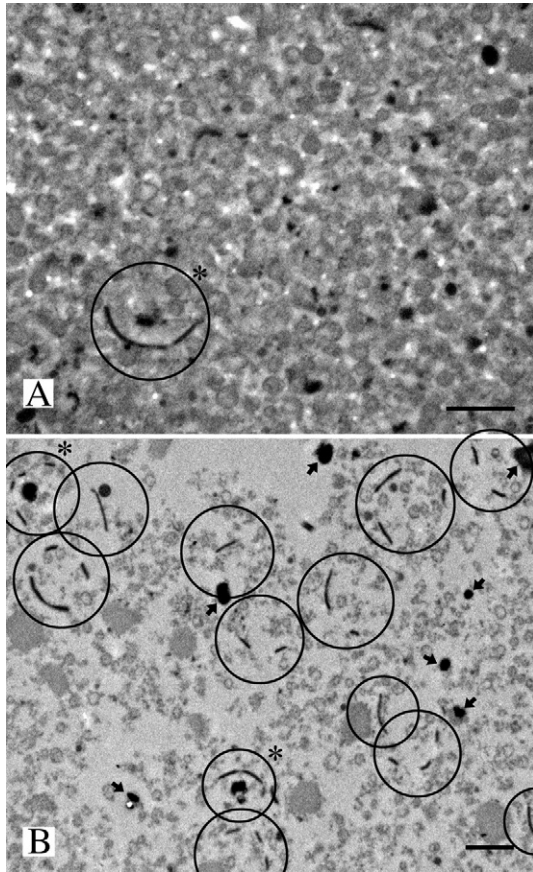


Fig. 4. Transmission electron micrographs of the subcellular fraction of *Rhizoctonia solani* isolated from above the 70% sucrose layer before (A) and after (B) treatment of the fraction with 2% Triton X-100 followed by centrifugation at 5000  $\times$ g for 1 h. Cell organelles other than septal pore caps (SPCs) (encircled) could not be identified. Few SPCs were co-purified with plugging material (\*). Arrows indicate possible isolated plugging material. Bar represents 1  $\mu$ m.

Mycelium of *R. solani* was subjected to high-pressure freezing (HPF) and freeze-substituted as described by Müller et al. (1998a). To subject the SPC-enriched fraction samples to HPF, an aluminum lecithin-coated planchette (100  $\mu$ m-deep well) used for HPF (Engineering Office M. Wohlwend) was dipped into the SPC-enriched pellet and we drew material from the bottom of the tube. A second lecithin-coated planchette (300  $\mu$ m-deep well) was placed with the flat side as a lid on top of the first planchette, thus subjecting 100  $\mu$ m thick SPC-enriched pellet material to HPF by the use of a Leica EM HPF (Leica Microsystems). After separating the planchettes in liquid nitrogen, the samples were freeze-substituted in a mixture of 1% (w/v) osmium tetroxide, 3% (v/v) glutaraldehyde, and 0.3% (w/v) uranyl acetate in anhydrous methanol at  $-85$   $^{\circ}$ C for two days. Finally, the samples were low-temperature embedded in lowicryl HM20 (Müller et al., 1991).

Sections of about 90 nm and 350 nm were cut with a diamond knife (Diatome) using an ULTRACUT E ultramicrotome (Leica Microsystems). The sections were picked up with formvar film-coated, carbon-stabilized copper grids (hexagonal 150 mesh Veco grids, EMS). Sections were contrasted with 4% (w/v) aqueous uranyl acetate (Merck) for 10 min and 0.4% (w/v) aqueous lead citrate (Merck) for 2 min (Venable and Coggeshall, 1965). The sections were viewed with a TECNAI 10 (FEI Company)

transmission electron microscopy at an acceleration voltage of 100 kV.

#### 2.4. Scanning electron microscopy

A small aliquot of the *R. solani* SPC-enriched fraction was placed on a formvar film-coated, carbon-stabilized grid and incubated for 10 min at room temperature. Thereafter, excess of fluid was removed carefully by touching the edge of the grid with a piece of Whatman paper, and subsequently the grid was air-dried overnight. Then, it was incubated 2 min with 4% (w/v) aqueous uranyl acetate, and subsequently washed thoroughly in distilled water. The grid was dried carefully with a piece of Whatman paper and further air-dried. Finally, the grids were mounted on a stub, coated with 5 nm Pt/Pd by using a Cressington sputter coater 208HR (Cressington Scientific Instruments), and viewed in a XL30 scanning electron microscopy (FEI Company) at an acceleration voltage of 15 kV and a working distance of about 8 mm.

### 3. Results

*R. solani* has dolipore septa with perforate SPCs of about 1.6–2.0  $\mu$ m in diameter as was observed in high-pressure frozen (HPF) and freeze-substituted mycelium examined by transmission electron microscopy (TEM) (Fig. 3). The dolipore channel may be open allowing passage of small organelles, i.e. mitochondria (Fig. 3A), or is plugged with electron-dense pore-occluding material (Fig. 3B). After two passages of 500 PSI (equivalent to 3447 kPa) through a French press, most of the harvested *R. solani* mycelium was broken as was examined by light microscopy (Fig. 2) and TEM (result not shown). The resulting cell homogenate was subjected to isopycnic centrifugation in a discontinuous 30–50–70% sucrose gradient. Cell walls were pelleted after centrifugation, while SPCs were mainly found on top of the 70% sucrose layer (Fig. 4A). Furthermore, many membrane vesicles were observed, and likely are formed as a result of the French press treatment to cell organelles and plasma- and vacuolar membranes. After treatment of this SPC-containing

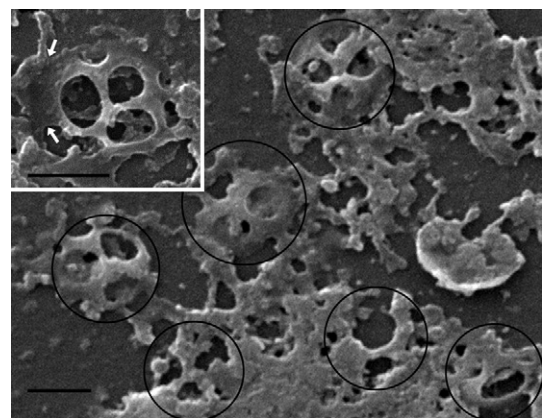


Fig. 5. Scanning electron micrographs of the septal pore cap-enriched fraction of *Rhizoctonia solani*. SPCs are encircled. The inset shows a higher magnification of an isolated SPC with putative endoplasmic reticulum attached at the base (arrows). Bar represents 1  $\mu$ m.

fraction with 2% Triton X-100, followed by centrifugation at  $5000 \times g$ , the amount of membrane vesicles was reduced and SPCs were further enriched (Fig. 4B). Few vesicles, but no SPCs were observed in the supernatants (result not shown).

Scanning electron microscopy showed that isolated SPCs were flattened and had a diameter of approximately  $1.5 \mu\text{m}$  and two to four perforations of about  $400\text{--}600 \text{ nm}$  (Fig. 5). Furthermore, the base of the SPC was continuous with membranes, which may be part of endoplasmic reticulum (ER) (Fig. 5, inset). TEM showed that thin-sectioned chemically fixed isolated SPCs maintained their characteristic dome-shaped structure after the enrichment procedure (Fig. 6) and could be co-isolated with occluding material (Fig. 6B–D). Additional structures that were necessary to retain the SPC dome-shape were not observed in SPCs isolated without plugging material (Fig. 6A). In the isolated complexes of SPC and occluding material, putative filaments occurred in between the SPC and the occluding material, which were visualized as a grey zone in chemical fixed SPC-enriched samples (Fig. 6B). An electron-translucent zone was visible between the

putative filaments and the inside of the SPC (Fig. 6B). To examine the ultrastructure of the isolated SPCs in more detail, SPC-enriched fractions from *R. solani* were fixed by HPF, followed by freeze-substitution. Examinations of these samples showed that isolated SPCs were connected to the occluding material by a filamentous network (Fig. 6C, D). Furthermore, HPF-fixed and freeze-substituted SPC-enriched samples gave a detailed view of the plug morphology that varied from loosely structured (Fig. 6C) to compact and densely structured (Fig. 6D). Between the inside of the SPC and the extensive filamentous network an amorphous layer was visible (Fig. 6C) that was less visible in the isolated SPC in Fig. 6D.

To investigate whether our method could be applied for the isolation of SPCs from other basidiomycete species, we subjected *T. cucumeris* and *C. cornigerum* to the combined use of French press and isopycnic centrifugation. SPCs of *T. cucumeris* and *C. cornigerum* are smaller than those of *R. solani* and are about  $1200 \text{ nm}$  and  $850 \text{ nm}$  in diameter respectively. Cell homogenates were successfully generated and for both, SPCs could be isolated

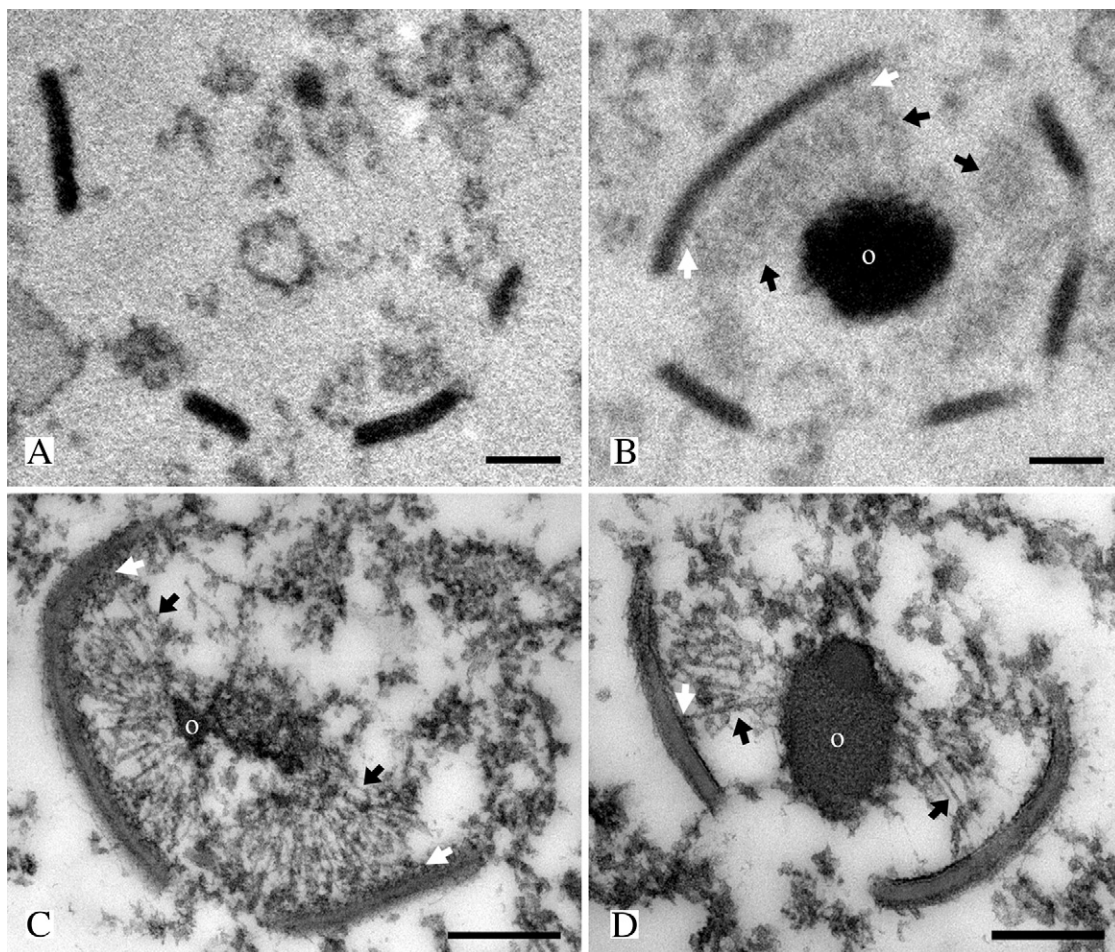


Fig. 6. Transmission electron micrographs of chemical fixed (A and B) or high-pressure frozen (HPF) and freeze-substituted (C and D) septal pore cap-enriched fractions of *Rhizoctonia solani*. A) Transverse section of an isolated SPC showing 3 perforations. B) Median section of an isolated SPC that is connected to electron-dense occluding material (o) via a putative filamentous network (black arrows). An electron-translucent zone is visible between the inside of the SPC and the filaments (white arrows). HPF-fixed and freeze-substituted SPC-enriched samples (C and D) show clearly the filamentous structures (arrows) that connect the electron-dense pore-occluding material (o) to the inside of the SPCs. Plug morphology varied from a loose structure (C), to a compact and dense structure (D). The plug with a loose structure (C) was connected to a more extensive filamentous network than the compact and dense structured plug (D). An amorphous layer is visible at the inside of the SPC (white arrows). Bar represents  $200 \text{ nm}$ .

after isopycnic centrifugation on top of the 70% sucrose layer (result not shown). However, the SPC-enriched fraction of *C. cornigerum* contained also mycelial fragments and remnants of broken cell walls, whereas *T. cucumeris* cell walls and mycelial fragments passed the 70% sucrose layer and were pelleted at the bottom of the ultracentrifuge tube, like in *R. solani* (result not shown). Moreover, *C. cornigerum* SPCs were also found in the 50% sucrose layer (result not shown). SPC fractions from *C. cornigerum* and *T. cucumeris* contained complexes of SPCs co-isolated with electron-dense occluding material as observed in *R. solani* SPC-enriched fractions (result not shown).

#### 4. Discussion

Fungal organelles can be isolated using several approaches. For example, *Penicillium chrysogenum* microbodies were isolated by protoplasting followed by isopycnic centrifugation (Müller et al., 1995b). Protoplasting does not affect the structural integrity of SPCs (Müller et al., 1998a), however, the yield of SPC-containing protoplasts is low and release of SPCs from protoplasts was unsuccessful (E. Boon and W.H Müller, unpublished results). Woronin bodies from *Neurospora crassa* were enriched after the cells were frozen in liquid nitrogen and ground to a fine powder that was separated on a sucrose cushion (Jedd and Chua, 2000). This study led to the findings that Woronin bodies are pre-formed peroxisomes that consist of HEX-1 protein and are necessary for septal pore sealing in ascomycetes (Jedd and Chua, 2000). More recently, laser microdissection by the use of a PALM laser beam system resulted into isolated septal regions of *R. solani* (Van Driel et al., 2007). Though fungal septa including SPCs were successfully isolated, laser microdissection is a very laborious technique that is not available in every laboratory. Furthermore, the isolation of proteins from sectioned fungal septa has not been optimized yet. Compared to described isolation methods, the success of our SPC isolation method is based on the combination of French press, isopycnic centrifugation, and Triton-X-100 that resulted into a high yield of isolated SPCs (Fig. 4B).

Cell homogenates of *R. solani*, *T. cucumeris*, and *C. cornigerum* were prepared by passage of the mycelium through a French press. We experienced that the smaller hyphae of *C. cornigerum* were more resistant to the pressure of the French press than the broader hyphae of *R. solani* and *T. cucumeris*, resulting in more mycelial fragments present in the fractions. Therefore, to generate cell homogenates from other fungi one may need additional passages or higher PSI values to break all the cells. By combining the French press with isopycnic centrifugation we could isolate the different sized SPCs as visualized by TEM. However, we cannot rule out that by the inclusion of the French press step in our method, parts of the SPCs will be ripped into smaller components that are not recognized in the SPC-enriched fraction by TEM. Still, when isolating these SPC-components together with the enriched intact SPCs, this will result into a high yield of SPC-components enhancing future biochemical studies.

To enrich the SPCs, we included a treatment with Triton X-100 detergent to solubilize the many membrane structures and vesicles that developed after French press treatment and isopycnic centrifugation. Triton X-100 is a non-ionic detergent often used

to solubilize lipid membranes to isolate membrane proteins or detergent-resistant membrane domains like lipid rafts (reviewed by London and Brown, 2000). Interestingly, this Triton-treatment did not solubilize the SPC-membranes, the filamentous network or the pore-occluding material as was only seen in the HPF-fixed and freeze-substituted SPC-enriched samples. Therefore, the membranes of the perforate SPCs of *R. solani* may not exclusively build-up by lipids that are solubilized by detergent, but they also may consist other components like sphingolipids or proteins that keep the SPC detergent-resistant. Wheat germ agglutinin labeling showed that *N*-acetyl glucosamine residues are present in SPCs (Benhamou et al., 1993; Van Driel et al., 2007) that may indicate the presence of glycoproteins in the SPC matrix, in the SPC-membranes or in both. Alternatively, a fibrous layer on top of the SPC (Fig. 6C and D) that was also observed in other studies (C.E. Bracker, pers. comm.; Müller et al., 2000a) and the amorphous layer at the inside of the SPC (Fig. 6C) that was also observed in *S. commune* (Müller et al., 1998a) may prevent SPC-membrane solubilization by Triton X-100.

Next to analysis of the fractions by TEM, SEM was used as a fast and easy-to-use method to analyze the quality of the SPCs and the degree of enrichment. SEM analysis showed that SPCs in the *R. solani* SPC-enriched fraction were slightly reduced in size and the characteristic dome-shaped morphology was flattened compared to earlier observations (Müller et al., 1998b). Both observations may be a result of the air-drying procedure in the preparation for SEM analysis. In contrast, TEM analysis showed isolated SPCs with the characteristic dome-shaped morphology. In addition, isolated SPCs that were not associated with plugging material did not show any additional structures that were necessary to retain the dome-shaped structure of SPCs as was proposed by Orlovich and Ashford (1994). This was also demonstrated in free-lying SPCs in *S. commune* protoplasts (Müller et al., 1998a), which showed the same morphology as in intact hyphal cells. These observations, together with the fact that the SPC structure was not broken down or solubilized after the enrichment procedure that includes passages through a French press and a Triton-treatment, we conclude that SPCs are resistant to high pressures and non-ionic surfactants.

The isolation of structural complexes consisting of SPCs connected to pore-occluding material by a filamentous network shows the close interaction of these two structures. Chemically fixed fractions showed an electron-translucent zone between the inside of the SPC and the filaments. We assume this zone is due to the preparation, because in HPF-fixed and freeze-substituted samples, an amorphous layer was visible instead, which agrees with previous observations (Müller et al., 1998a). This may be material from the SPC that contributes to the build-up of filaments or pore-occluding material. We, however, cannot rule out that during the isolation method proteins may be trapped into this zone due to the many filaments that are present (Fig. 6C). When few filaments are present, these proteins then can be easily washed off (Fig. 6D). The filamentous network between SPCs and occluding material agrees with previously reported observations of SPCs in intact hyphae after automated electron tomography (Müller et al., 2000a). The filamentous connections between SPCs and pore-occluding material and the isolation of

these three structures as a structural complex suggest that SPCs may take part in the plugging process of dolipores and thereby fulfill a crucial role in maintaining cell homeostasis. Furthermore, the filamentous network showed dynamics in density and was found to be more extensive when the plug was loosely structured (Fig. 6C) instead of compact (Fig. 6D). In addition, those parts of the SPC that are connected with the filaments show a less electron-dense SPC matrix than the remainder of the SPC matrix (Müller et al., 2000a). This indicates that the filaments between SPC and occluding material may be involved in the formation of pore-occluding material.

## Acknowledgements

I would like to thank M. Smith and G. Poot for instructions on the French press and the ultracentrifuge, respectively, and C. Schneijdenberg and H. Meeldijk for instructions on the transmission electron microscopy. This work was financially supported by the Odo van Vloten foundation.

## References

- Aylmore, R.C., Wakley, G.E., Todd, N.K., 1984. Septal sealing in the basidiomycete *Coriolus versicolor*. J. Gen. Microbiol. 130, 2975–2982.
- Benhamou, N., Broglie, K., Broglie, R., Chet, I., 1993. Antifungal effect of bean chitinase on *Rhizoctonia solani*: ultrastructural changes and cytochemical aspects of chitin breakdown. Can. J. Microbiol. 39, 318–328.
- Bracker, C.E., Butler, E.E., 1963. The ultrastructure and development of septa in hyphae of *Rhizoctonia solani*. Mycologia 55, 35–58.
- Bracker, C.E., Butler, E.E., 1964. Function of the septal pore apparatus in *Rhizoctonia solani* during protoplasmic streaming. J. Cell Biol. 21, 152–157.
- Girbardt, M., 1958. Über die Substruktur von *Polystictus versicolor*. Arch. Mikrobiol. 28, 255–269.
- Girbardt, M., 1961. Licht-und-elektronen-mikroskopische Untersuchungen an *Polystictus versicolor*. II. Die Feinstruktur von Grundplasma und Mitochondrien. Arch. Mikrobiol. 39, 351–359.
- Gull, K., 1978. In: Smith, J.E. (Ed.), Form and function of septa in filamentous fungi. The filamentous fungi: developmental mycology, vol. 3. Edward Arnold, London, UK, pp. 78–93.
- Jedd, G., Chua, N.-H., 2000. A new self-assembled peroxisomal vesicle required for efficient resealing of the plasma membrane. Nat. Cell Biol. 2, 226–231.
- London, E., Brown, D.A., 2000. Insolubility of lipids in Triton X-100: physical origin and relationship to sphingolipid/cholesterol membrane domains (rafts). Biochim. Biophys. Acta 1508, 182–195.
- Markham, P., 1994. Occlusions of septal pores in filamentous fungi. Mycol. Res. 98, 1089–1106.
- McLaughlin, D.J., Frieders, E.M., Lü, H., 1995. A microscopist's view of heterobasidiomycete phylogeny. Stud. Mycol. 38, 91–109.
- Moore, R.T., McAlear, J.H., 1962. Fine structure of Mycota. 7. Observations on septa of ascomycetes and basidiomycetes. Am. J. Bot. 49, 86–94.
- Müller, W.H., Van der Krift, T.P., Knoll, G., Smaal, E.B., Verkleij, A.J., 1991. A preparation method of specimens of the fungus *Penicillium chrysogenum* for ultrastructural and immuno-electron microscopical changes. J. Microsc. 169, 29–41.
- Müller, W.H., van Aelst, A.C., van der Krift, T.P., Boekhout, T., 1995a. Novel approaches to visualize the septal pore cap. Stud. Mycol. 38, 111–117.
- Müller, W.H., Essers, J., Humbel, B.M., Verkleij, A.J., 1995b. Enrichment of *Penicillium chrysogenum* microbodies by isopycnic centrifugation in nycodenz as visualized with immuno-electron microscopy. Biochim. Biophys. Acta 1245, 215–220.
- Müller, W.H., Montijn, R.C., Humbel, B.M., van Aelst, A.C., Boon, E.J.M.C., van der Krift, T.P., Boekhout, T., 1998a. Structural differences between two types of basidiomycete septal pore caps. Microbiology 144, 1721–1730.
- Müller, W.H., Stalpers, J.A., van Aelst, A.C., van der Krift, T.P., Boekhout, T., 1998b. Field emission gun-scanning electron microscopy of septal pore caps of selected species in the *Rhizoctonia* s.l. complex. Mycologia 90, 170–179.
- Müller, W.H., Koster, A.J., Humbel, B.M., Ziese, U., Verkleij, A.J., van Aelst, A.C., van der Krift, T.P., Montijn, R., Boekhout, T., 2000a. Automated electron tomography of the septal pore cap in *Rhizoctonia solani*. J. Struct. Biol. 131, 10–18.
- Müller, W.H., Stalpers, J.A., van Aelst, A.C., de Jong, M.D.M., van der Krift, T.P., Boekhout, T., 2000b. The taxonomic position of *Asterodon*, *Asterostroma* and *Coltricia* inferred from the septal pore cap ultrastructure. Mycol. Res. 104, 1485–1491.
- Orlovich, D.A., Ashford, A.E., 1994. Structure and development of the dolipore septum in *Pisolithus tinctorius*. Protoplasma 178, 66–80.
- Patrignani, G., Pellegrini, S., 1986. Fine structures of the fungal septa on varieties of basidiomycetes. Caryologia 39, 239–250.
- Rieder, S.E., Emr, S.D., 2000. Isolation of subcellular fractions from the yeast *Saccharomyces cerevisiae*. In: Bonifacino, J.S., Dasso, M., Lippincott-Schwartz, J., Harford, J.B., Yamada, K.M. (Eds.), Current protocols in cell biology. John Wiley and Sons, NY, p. 3.8.45.
- Spurr, A.R., 1969. A low viscosity resin embedding medium for electron microscopy. J. Ultrastruct. Res. 26, 31–43.
- Van Driel, K.G.A., Boekhout, T., Wösten, H.A.B., Verkleij, A.J., Müller, W.H., 2007. Laser microdissection of fungal septa as visualized by scanning electron microscopy. Fungal Genet. Biol. 44, 173–466.
- Venable, J.H., Coggeshall, R., 1965. A simplified lead citrate stain for use in electron microscopy. J. Cell Biol. 25, 407–408.
- Wilsenach, R., Kessel, M., 1965. On the function and the structure of the septal pore of *Polyporus rugulosus*. J. Gen. Microbiol. 40, 397–400.